

# artikel 5

*by* Rahmat Doni Widodo

---

**Submission date:** 08-May-2022 08:48AM (UTC+0700)

**Submission ID:** 1830869346

**File name:** 5-Widodo\_2021\_IOP\_Conf.\_Ser.\_Earth\_Environ.\_Sci.\_700\_012001.pdf (838.63K)

**Word count:** 5134

**Character count:** 29054

PAPER · OPEN ACCESS

## Shrinkage, Density and Hardness of Hard Magnetic Material (BaFe<sub>12</sub>O<sub>19</sub>) Based on Iron Sand Produced by Conventional Solid-State Reaction Process

To cite this article: R D Widodo *et al* 2021 *IOP Conf. Ser.: Earth Environ. Sci.* **700** 012001

6  
View the [article online](#) for updates and enhancements.



**240th ECS Meeting** ORLANDO, FL

Orange County Convention Center Oct 10-14, 2021

Abstract submission due: April 9

SUBMIT NOW

## Shrinkage, Density and Hardness of Hard Magnetic Material (BaFe<sub>12</sub>O<sub>19</sub>) Based on Iron Sand Produced by Conventional Solid-State Reaction Process

R D Widodo<sup>1\*</sup>, Priyono<sup>2</sup>, Rusiyanto<sup>1</sup>, S Anis<sup>1</sup>, R I Ilham<sup>1</sup>, H N Firmansyah<sup>1</sup>, N Wahyuni<sup>3</sup>

<sup>1</sup> Department of Mechanical Engineering, Faculty of Engineering, Universitas Negeri Semarang (UNNES), Gunungpati Current Campus, Semarang, Indonesia.

<sup>2</sup> Department of Physics, Faculty of Mathematics and Natural Sciences, University of Diponegoro, Tembalang Campus, Semarang, Indonesia.

<sup>3</sup> Department of Automotive Engineering, Politeknik Negeri Ujung Pandang, South Sulawesi, Indonesia.

rahmat\_doni@mail.unnes.ac.id

**Abstract.** This paper presents shrinkage, density and hardness number of hard magnetic (BaFe<sub>12</sub>O<sub>19</sub>) based on iron sand produced by conventional solid-state reaction process. Iron sand was mechanically filtered using permanent magnets 35 times. The filtered iron sand was heated at temperatures of 900°C for 5 hours in the furnace and after it was cold and produce Fe<sub>2</sub>O<sub>3</sub> phase. Powders of Fe<sub>2</sub>O<sub>3</sub> and BaCO<sub>3</sub> were mixed and milled in a shaker ball mill up to 3 hours. The powder mixture compacted at a pressure of 2.5, 5 and 7.5 tons and followed by sintering at temperature of 1100, 1150 and 1200°C for 1 hour in the furnace. Shrinkage measurements include diameter and height uses vernier caliper, while density measurements use the Archimedes method. Hardness number obtained with pass vickers hardness testing methods. Barium ferrite 's maximum shrinkage and bulk density values were at 7.5 tons compacting pressure and 1200°C sintering temperature where the shrinkage value was 7.44 percent, average shrinkage was 3.49 percent, and density was 4.397 g/cm<sup>3</sup>. In barium ferrite with a compacting pressure of 7.5 tons and a sintering temperature of 1200 °C which is equivalent to 741 HV the highest hardness value is found. The higher the compacting press and sintering temperature, the greater the importance of bulk density and hardness of the materials.

### 1. Introduction

The large amount of iron sand found in the south coast of Java has the great potential to be a special hard magnetic base material and is generally adopted as a base for electronic components [1-3]. Iron sand in general has a dominant chemical compound such as magnetite (Fe<sub>3</sub>O<sub>4</sub>), maghemite (γ-Fe<sub>2</sub>O<sub>3</sub>) dan hematite (α-Fe<sub>2</sub>O<sub>3</sub>) [4-7]. Magnetite (Fe<sub>3</sub>O<sub>4</sub>) is the mineral that has the highest iron content, that hits up to 72.4% [8]. This mineral is known to have the strongest magnetic properties. Thus, it is also known as Lodstone (magnetic stone) [9]. Magnetite is used as the main ingredient of iron ore in the manufacture of steel and iron [8]. At the nanometer scale, the material with this magnetite compound has superparamagnetic properties and has other properties such as saturation magnetization, biological compatibility and environmental stability which are better when compared to the size on the bulk scale [10-14].

Maghemite (γ-Fe<sub>2</sub>O<sub>3</sub>) is a strongly ferrimagnetic which has the same crystal structure with magnetite and similar chemical composition with hematite but has a different crystal structure where the maghemite has a crystal cubic structure and hematite has a hexagonal crystal structure [15-20]. Maghemites in natural environment are typically formed by the process of oxidation of magnetite at low temperatures [15,17]. Compared with magnetite the presence of maghemites in natural environment is very small. The cycle of oxidation (addition of oxygen) by giving heat to magnetite at certain temperatures becomes maghemite and hematite [21-25]. Maghemite produced through the magnetite oxidation process is characterized by a color shift from black to reddish brown [26-29]. Maghemite is widely applied in the biomedical field [30-



35], magnetic recording media [36] and nanoparticle technology, namely in the treatment of cancer cells in hyperthermia [37-38].

Hematite is the mineral form of iron (III) oxides ( $\alpha\text{-Fe}_2\text{O}_3$ ) which are antiferro magnetic or in other words hematite is not magnetic and should not respond to a common magnet. However, many specimens of hematite contain enough magnetite that they are attracted to a common magnet [39]. Iron (III) oxides ( $\alpha\text{-Fe}_2\text{O}_3$ ) can be synthesized using different techniques including co-precipitation method [40], thermal decomposition [41-43], hydrothermal synthesis [10, 14, 44, 45], microemulsion [46, 47], and sonochemical synthesis [48, 49]. Iron (III) oxides ( $\alpha\text{-Fe}_2\text{O}_3$ ) are used more commonly for the manufacture of pigments, products for radiation control, ballasts, solar cells, microwave absorption, catalysis, environmental protection, gas sensors, magnetic storage, clinical diagnosis and treatment, etc [39, 50-54]. Iron (III) oxides ( $\alpha\text{-Fe}_2\text{O}_3$ ) are more commonly used as a base material for ferrite magnets that have hard magnetic properties [55]. The magnetic properties of iron (III) oxides ( $\alpha\text{-Fe}_2\text{O}_3$ ) were demonstrated to depend on their size, shape and microstructure [45, 56]. Iron (III) oxides ( $\alpha\text{-Fe}_2\text{O}_3$ ) are an enticing category of products, ranging from antiferromagnetic, superparamagnetic and bulky ferromagnetic to ferrimagnetic [57, 58]. When the particle size decreases, the magnetic properties of iron (III) oxides ( $\alpha\text{-Fe}_2\text{O}_3$ ) have unusual properties that vary from those of bulk equivalents due to nanoscale concentration and surface impact [56, 59].

Iron (III) oxides ( $\alpha\text{-Fe}_2\text{O}_3$ ) are more commonly used in ferrite magnets with hard magnetic properties as the base material. Ferrite magnets can generally be made using compound Iron (III) oxides added by  $\text{BaCO}_3$  to manufacture barium hexaferrite magnets and  $\text{SrCO}_3$  to produce strontium hexaferrite magnets [60-62]. The magnetic properties of ferrite are influenced by several factors including the level of purity and types of constituent compounds, stoichiometry, crystallite size, microstructure, preparation and manufacturing processes [63]. The process of preparing and producing ferrite magnets can be accomplished using many techniques or methods, including sol-gel, coprecipitation, salt-melting, citrate, hydrothermal, combustion, high-temperature self-propagation and normal ceramic techniques (solid-state reaction, mechanical milling and alloying) [63].

The process of making ferrite magnets, especially barium hexaferrite using standard ceramic techniques, where  $\text{Fe}_2\text{O}_3$  and  $\text{BaCO}_3$  powders are processed by mechanical milling and alloying followed by a sintering process. This process is also commonly referred to as the solid-state reaction process, where during the sintering process a reaction occurs between  $\text{Fe}_2\text{O}_3$  and  $\text{BaCO}_3$  resulting in barium hexaferrite ( $\text{Ba}_0.6\text{Fe}_{12}\text{O}_{19}$  or  $\text{BaFe}_{12}\text{O}_{19}$ ). Before the sintering process is carried out, the samples are given emphasis treatment (compacting) and some are not. Things that need to be considered before, during and after the sintering process include the heating rate, temperature variations, atmosphere, holding time and cooling rate which will affect the  $\text{BaFe}_{12}\text{O}_{19}$  microstructure [63]. Microstructure material affects many things such as physical, mechanical, magnetic etc. Many solid-state reaction processes are carried out because they have advantages including mass production, are easy, simple, inexpensive and can produce nanoparticles [64, 65]. This research reports the effect of compacting pressure and sintering temperature on shrinkage, bulk density and hardness number on  $\text{BaFe}_{12}\text{O}_{19}$  hard magnetic material based on iron sand by solid-state reaction process.

## 2. Experiments

Iron sand from Ketawang Indah beach with permanent magnetic rocks from Purworejo is mechanically extracted 35 times. The iron sand removed was then oxidized over 5 hours at a heating temperature of  $900^\circ\text{C}$ . Iron oxide and barium carbonate ( $\text{BaCO}_3$ ) were weighed for based on stoichiometry calculations and then followed by mechanical alloying and milling treatment using a shaker ball mill for 3 hours.

After the mechanical alloying and milling process the mixture of  $\text{Fe}_2\text{O}_3$  and  $\text{BaCO}_3$  powders was molded with compacting pressure variation; 2.5, 5 and 7.5 tons where the diameter of the dies is 2 cm. The sample of compacting or green compact is measured in diameter and height dimensions using Mitutoyo Vernier Caliper Metric with an accuracy of 0.05 mm. Then the green compact sample was sintered with variations in temperature of  $1100^\circ\text{C}$ ,  $1150^\circ\text{C}$ , and  $1200^\circ\text{C}$  for 1 hour using furnace (Nabertherm N31/H) until room temperature. The sample is measured shrinkage which includes shrinkage of diameter and height using vernier caliper and then calculated using the given equation 1 and 2.

$$\Delta d = \frac{d_1 - d_2}{d_1} \times 100 \% \quad (1)$$

$$\Delta h = \frac{h_1 - h_2}{h_1} \times 100 \% \quad (2)$$

Where,  $\Delta d$  = diameter shrinkage (%);  $\Delta h$  = high shrinkage (%);  $d_1$  = diameter of the sample before sintering (mm);  $d_2$  = diameter of the sample after sintering (mm);  $h_1$  = sample height before sintering (mm); and  $h_2$  = sample height after sintering (mm).

Bulk density sample measurements were done after the sintering process using the Archimedes method [66]. Whilst the material's hardness value was measured using the Vickers method using the M800 microhardness tool with a load of 100 gf held for 10 seconds.

### 3. Result and discussion

#### 3.1. Shrinkage

Depreciation testing on samples is done on the dimensions of diameter ( $\Delta d$ ) and specimen height ( $\Delta h$ ). The results of diameter shrinkage test ( $\Delta d$ ) with variations in compacting pressure and sintering temperature as shown in the Figure 1.

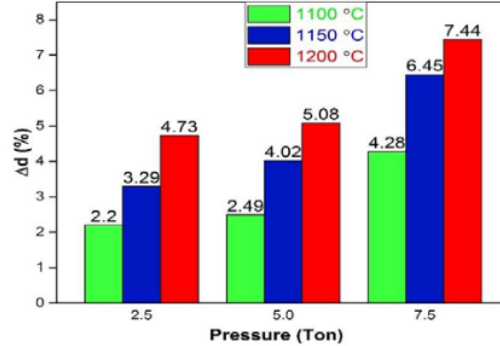


Figure 1. Shrinkage of diameter ( $\Delta d$ )

Figure 1 shows a significant increase in diameter shrinkage of the specimen when treated with variations in compacting pressure and sintering temperature. The test results show that the specimens treated with 2.5 ton compacting pressure and sintering temperature of 1100°C had the smallest diameter shrinkage value of 2.2%. In the sintering treatment 1150°C has a diameter shrinkage value of 3.29%. Whereas the 1200°C sintering treatment has a diameter shrinkage value of 4.37%. The increase in the value of diameter shrinkage that occurs at a pressure of 2.5 tons along with the increase in sintering temperature is around 1.09-2.17%. For specimens treated with 5 ton compacting pressure, the magnitude of the diameter depreciation is not adrift with diameter shrinkage values for specimens treated with 2.5 ton compacting pressure at each sintering temperature. The largest diameter shrinkage value in the specimen which was given a compacting pressure of 7.5 tons in each sintering treatment, especially in the 1200°C sintering treatment which has the largest diameter shrinkage value of 7.44%. The value of diameter shrinkage that occurs at a pressure of 7.5 tons at each variation of the sintering temperature is 2.17-3.16%. This indicates that the higher the compacting pressure and sintering temperatures cause the denser conditions of the specimen.

The results of high shrinkage test ( $\Delta h$ ) samples with variations in compacting pressure and sintering temperature as shown in Figure 2.

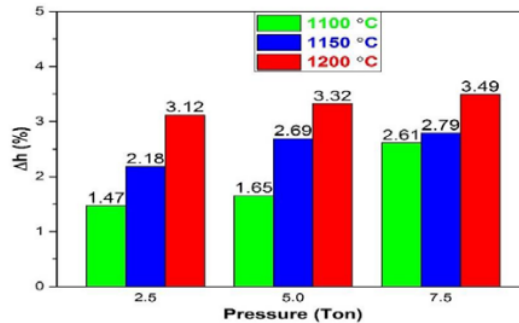


Figure 2. Shrinkage of high ( $\Delta h$ )

In Figure 2, it can be seen that the specimens given a 2.5 ton compacting pressure treatment and sintering temperature of 1100°C have the smallest high shrinkage value of 1.47%. While the highest high shrinkage value is owned by the specimen with a compacting pressure of 7.5 tons and a sintering

temperature of 1200°C which is 3.49%. The graph trend in Figure 2 is almost the same as the graph trend in Figure 1, where the cause of the phenomenon is that the higher the pressure and sintering temperature to 1200°C causes the denser conditions of the specimen and the lower the specimen's ability to return to its original dimensions after sintering. In microstructure this happens due to the diffusion process (mass transposition) of atoms between particles resulting in the growth of grains and eliminating pores in the specimen. High shrinkage speed can affect the characteristics of the sintering material, where the uneven distribution of sintering temperatures can cause residual stresses that are the source of cracks [67-70].

### 3.2. Bulk Density Measurement

The results of bulk density testing in samples with variations in compacting pressure and sintering temperature can be seen in Figure 3. In Figure 3 it is clear that the specimens which are compacted at 7.5 tons and sintered at 1200 °C have the highest bulk density values of 4.4 g/cm<sup>3</sup>. Overall the increase in the value of bulk density that occurs along with the increase in compacting pressure and sintering temperature is around 0.091-0.186%.

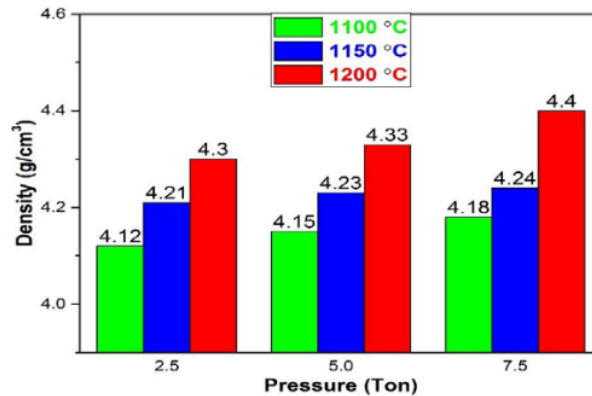


Figure 3. Bulk density

Research conducted by Kristiantoro et.al (2019) got a bulk density value of 4.65 g/cm<sup>3</sup>, where the increasing value of density also increases the value of remanence (Br) and maximum product energy (BHmax), but further decreases the value of coercivity (Hc) [71]. The highest barium hexaferrite bulk density value ever achieved in previous studies was reported at 5,295 g/cm<sup>3</sup> [63], while the theoretical density of barium hexaferrite is 5.32 g/cm<sup>3</sup> [72]. When compared with the highest bulk density value ever obtained and the theoretical density value of the results obtained in this study, the value is still smaller, this is due to the possibility that there are still many pores in the specimen even though this research has not been explored further on this subject. The application of higher compacting pressure and sintering at a temperature of 1200°C allows the particles in the specimen to disperse and the particle growth occurs during the sintering process thus reducing the pores in the specimen and this also allows the volume of the specimen to shrink [73].

### 3.3. Hardness testing

The results of hardness testing on the variation of compacting pressure and sintering temperature can be seen in Figure 4. Figure 4 shows that the test results show that the specimens have the lowest test hardness value of 255 HV despite a compacting pressure treatment and sintering temperature of 1100°C. Whereas the highest check hardness value belongs to the specimen with a compacting pressure of 7.5 tons and a sintering temperature of 1200°C which is 741 HV.

In the research of Kristiantoro et.al (2019) obtained a hardness value of 42.5 HRC or around 420 HV at a compacting pressure of 6 tons/cm<sup>2</sup> which is sintered 1250°C [71]. It can be concluded that the greater compacting pressure and sintering temperature would induce a higher hardness value. This is because the higher the compacting pressure applied to the specimen, the bonding of particle granules becomes stronger in order to increase or decrease the distance between particles. If the particle granules get thicker then the particles would be easier to bind during the sintering process, thus as to improve the material's hardness value.

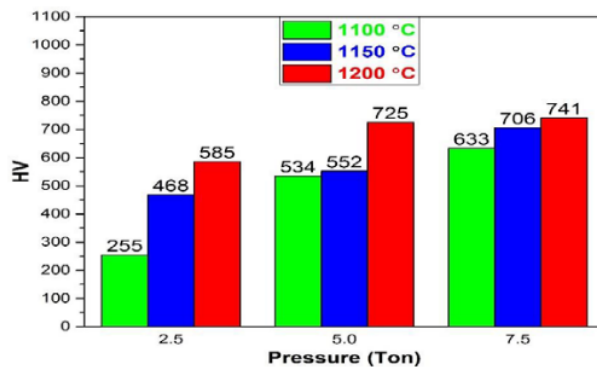


Figure 4. Vickers hardness number

#### 8 4. Conclusion

Based on the research that has been done, the following conclusions can be drawn: Compacting pressure and sintering temperature affect the value of shrinkage and density of hard magnet barium ferrite-based iron sand, where the higher the compacting pressure and sintering temperature, the shrinkage value and material density will increase. The highest shrinkage and density values were found in barium ferrite with the treatment of compacting pressure of 7.5 tons and sintering temperature of 1200°C, with diameter shrinkage of 7.44%, high shrinkage of 3.49%, and density value of 4.397 g/cm<sup>3</sup>.

The compacting pressure and sintering temperature affect the hardness of barium ferrite magnets based on iron powder. The higher the compacting press and sintering temperature, the greater the significance of material hardness. For barium ferrite with a compacting pressure of 7.5 tons and a sintering temperature of 1200°C which is equivalent to 741 HV the maximum hardness value is found.

#### Acknowledgement

We thank to Engineering Faculty, Semarang State University for the support of laboratory facilities and funding. This research was funded from the DIPA Number: 023.17.2.677507/2020 through the collaborative research scheme. We also thank the Department of Physics, Faculty of Mathematics and Natural Sciences, University of Diponegoro for supporting the laboratory facilities.

#### References

- [1] Andimutiafitri 2018 Synthesis of Magnetite Based Iron Sand by Using Coprecipitation method *IOSR-Journal of Applied Physics (IOSR-JAP)* **10** 40-42
- [2] Rianna M, Sembiring T, Situmorang M, Kurniawan C, Setiadi EA, Tetuko AP, Simbolon S, Ginting M, Sebayang P 2018 Preparation and Characterization of Natural Iron Sand from Kata Beach, Sumatera Barat Indonesia with High Energy Milling (HEM) *Jurnal Natural* **18** 97-100
- [3] Widodo R D, Priyono, Rusiyanto, Anis S, Ichwani A A, Setiawan B, Fitriyana D F and Rochman L 2020 Synthesis and Characterization of Iron (III) Oxide from Natural Iron Sand of The South Coastal Area Purworejo Central Java *Journal of Physics: Conference Series* **1444** 012043
- [4] Manjunatha M, Kumar R, Anupama A V, Khopkar V B, Damle R, Ramesh K P, Sahoo B 2019 XRD, Internal Field-NMR and Össbauer Spectroscopy Study of Composition, Structure and Magnetic Properties of Iron Oxide Phases in Iron Ores *Journal of Materials Research and Technology* **8** 2192-2200
- [5] Muflikhah, Rusdiarso B, Putra E G R, Nuryono 2017 Modification of Silica Coated on Iron Sand Magnetic Material with Chitosan for Adsorption of Au(III) *Indonesian Journal of Chemistry* **17** 264-273
- [6] Sehah, Raharjo S A, Kurniawan M A 2016 Distribution of Iron Sand in the Widarapayung Coast Area at Regency of Cilacap Based on Magnetic Anomaly Data *Indonesian Journal of Applied Physics* **6** 97-106
- [7] Fahlepy M R, Wahyuni Y, Andhika M, Tiwow V A, Subaer 2019 Synthesis and Characterization of Nanoparticle Hematite ( $\alpha$ -Fe<sub>2</sub>O<sub>3</sub>) Minerals from Natural Iron Sand Using Co-Precipitation Method and its Potential Applications as Extrinsic Semiconductor Materials Type-N *Materials Science Forum* **967** 259-266
- [8] Glenn D Considine 2005 Iron. Van Nostrand's Encyclopedia of Chemistry, 5th Edition John Wiley

- & Sons, Inc
- [9] Setyawan H and Widiyastuti W 2019 Progress in the Preparation of Magnetite Nanoparticle through the Electrochemical Method *KONA Powder and Particle Journal* **36** 145-155
- [10] Saragi T, Santika A S, Permana B, Syakir N, Khartawidjaja M and Risdiana 2017 Synthesis and Properties of Iron Oxide Particles Prepared by Hydrothermal Method. *Journal of Physics: Conference Series: Material Science and Engineering* **196** 012025
- [11] Fuentes-Garcia J A, Diaz-Cano A I, Guillen-Cervantes A and Santoyo-Salazar J 2018 Magnetic Domain Interactions of Fe<sub>3</sub>O<sub>4</sub> Nanoparticles Embedded in a SiO<sub>2</sub> Matrix *Scientific Reports* **8** 5096
- [12] Tartaj P, Morales M P, Gonzalez-Carreno T, Veintemillas-Verdaguer S, Serna C J 2005 Advances in Magnetic Nanoparticles Biotechnology Applications *Journal of Magnetism and Magnetic Materials* **290** 28–34
- [13] Peter Majewski and Benjamin Thierry 2007 Functionalized Magnetite Nanoparticles-Synthesis, Properties, and Bio-Applications *Critical Reviews in Solid State and Materials Sciences* **32** 203-215
- [14] Islam M S, Kurawaki J, Kusumoto Y, Abdulla-Al-Mamun M and Bin Mukhlsh M Z 2012 Hydrothermal Novel Synthesis of Neck-structured Hyperthermia-suitable Magnetic (Fe<sub>3</sub>O<sub>4</sub>, γ-Fe<sub>2</sub>O<sub>3</sub> and α-Fe<sub>2</sub>O<sub>3</sub>) *Nanoparticles Journal of Scientific Research* **4** 99-107
- [15] Cor B de Boer and Dekkers M J 1996 Grain-size Dependence of The Rock Magnetic Properties for a Natural Maghemite *Geophysical Research Letters* **23** 2815-2818
- [16] Ling Hu, Aurelien Percheron, Denis Chaumont and Claire-Helene Brachais 2011 Microwave-Assisted One-Step Hydrothermal Synthesis of Pure Iron Oxide Nanoparticles: Magnetite, Maghemite and Hematite Search Results *Journal of Sol-Gel Science and Technology* **60** 198–205
- [17] Chirita M and Grozescu I 2009 Fe<sub>2</sub>O<sub>3</sub>– Nanoparticles, Physical Properties and Their Photochemical and Photoelectrochemical Applications *Chemical Bulletin "POLITEHNICA" Univ. (Timisoara)* **54** 1-8
- [18] Komorida Y, Mito M, Deguchi H, Takagi S, Tajiri T, Silva N JO, Laguna M A, Palacio F and Milla A 2010 Effects of Pressure on Maghemite Nanoparticles with a Core/Shell Structure *Journal of Magnetism and Magnetic Materials* **322** 2117–2126
- [19] Shokrollahi H 2017 A Review of The Magnetic Properties, Synthesis Methods and Applications of Maghemite *Journal of Magnetism and Magnetic Materials* **426** 74–81
- [20] Coduri M, Masala P, Bianco LD, Spizzo F, Ceresoli D, Castellano C, Cappelli S, Oliva C, Checchia S, Allieta M, Szabo D-V, Schlabach S, Hagelstein M, Ferrero C and Scavini M 2020 Local Structure and Magnetism of Fe<sub>2</sub>O<sub>3</sub> Maghemite Nanocrystals: The Role of Crystal Dimension *Nanomaterials* **10** 867
- [21] Khan UM, Amanullah, Manan A, Khan N, Mahmood A and Rahim A 2015 Transformation Mechanism of Magnetite Nanoparticles *Materials Science-Poland* **33** 278-285
- [22] Ghufuron M, Baqiya MA, Mashuri, Triwikantoro and Darminto 2011 Phase Transition in Fe<sub>3</sub>O<sub>4</sub>/Fe<sub>2</sub>O<sub>3</sub> Nanocomposites By Sintering Process *Indonesian Journal of Materials Science* **12** 120 - 124
- [23] Bertrand N, Desgranges C, Poquillon D, Lafont M C and Monceau D 2009 Iron Oxidation at Low Temperature (260–500 C) in Air and the Effect of Water Vapor *Oxidation of Metals* **73** 139-162
- [24] Li Z, Chan C, Berger G, Delaunay S, Graff A and Lefevre G 2019 Mechanism and Kinetics of Magnetite Oxidation under Hydrothermal Conditions *RSC Advances* **9** 33633–33642
- [25] Cuenca JA, Bugler K, Taylor S, Morgan D, Williams P, Bauer J and Porch A 2016 Study of the Magnetite to Maghemite Transition Using Microwave Permittivity and Permeability Measurements *Journal of Physics: Condensed Matter* **28** 106002
- [26] Kazeminezhad I and Mosivand S 2014 Phase Transition of Electrooxidized Fe<sub>3</sub>O<sub>4</sub> to γ and α-Fe<sub>2</sub>O<sub>3</sub> Nanoparticles Using Sintering Treatment *Acta Physical Polonica A* **125** 1210-1214
- [27] Wahyuningsih S, Ramelan AH and Kristiawan YR 2019 Transformation of Magnetite (Fe<sub>3</sub>O<sub>4</sub>) and Maghemite (γ-Fe<sub>2</sub>O<sub>3</sub>) to α-Fe<sub>2</sub>O<sub>3</sub> from Magnetic Phase of Glagah Iron Sand *Journal of Engineering Science* **15** 11–21
- [28] Katikaneani P, Vaddepally AK, Tippana NR, Banavath R, and Kommu S 2016 Phase Transformation of Iron Oxide Nanoparticles from Hematite to Maghemite in Presence of Polyethylene Glycol: Application as Corrosion Resistant Nanoparticle Paints *Journal of Nanoscience* **2016** 1328463
- [29] Vella L and Emerson D 2012 Electrical Properties of Magnetite and Hematite-Rich Rocks and Ores *ASEG Extended Abstracts* **1** 1-4
- [30] Kour S, Sharma RK, Jasrotia R, and Singh VP 2019 A Brief Review on the Synthesis of Maghemite



- ( $\gamma$ -Fe<sub>2</sub>O<sub>3</sub>) for Medical Diagnostic and Solar Energy Applications *AIP Conference Proceedings* **2142** 090007
- [31] Ali LMA, Piñol R, Villa-Bellosta R, Gabilondo L, Millán A, Palacio F and Sorribas V 2015 Cell Compatibility of a Maghemite/Polymer Biomedical Nanoplatform *Toxicology in Vitro* **29** 962–975
- [32] Raman M, Devi V and Doble M 2015 Biocompatible  $\iota$ -Carrageenan- $\gamma$ -Maghemite Nanocomposite for Biomedical Applications –Synthesis, Characterization and in Vitro Anticancer Efficacy *Journal of Nanobiotechnology* **13** 18
- [33] Yousefi A, Seyyed Ebrahimi S A, Seyfoori A and Mahmoodzadeh Hosseini H 2017 Maghemite Nanorods and Nanospheres: Synthesis and Comparative Physical and Biological Properties *BioNanoScience* **8** 95–104
- [34] Felix A, Blyakhman, Alexander P, Safronov, Andrey Yu, Zubarev, Tatyana F, Shklyar, Oleg G, Makeyev, Emilia B, Makarova, Vsevolod V, Melekhin, Aitor Larrañaga and Galina V. Kurlyandskaya 2017 Polyacrylamide Ferrogels with Embedded Maghemite Nanoparticles for Biomedical Engineering *Results in Physics* **7** 3624–3633
- [35] Abeer A, Abd Elrahman and Fotouh R, Mansour 2019 Targeted Magnetic Iron Oxide Nanoparticles: Preparation, Functionalization and Biomedical Application *Journal of Drug Delivery Science and Technology* **52** 702–712
- [36] Richard Dronskowski 2001 The Little Maghemite Story: A Classic Functional Material *Advanced Functional Materials* **11** 27-29
- [37] Múzquiz-Ramos E M, Guerrero-Chávez V, Macías-Martínez B I, López-Badillo C M and García-Cerda L A 2015 Synthesis and Characterization of Maghemite Nanoparticles for Hyperthermia Applications *Ceramics International* **41** 397–402
- [38] Singh M, Ramanathan R, Mayes ELH, Masková S, Svoboda P and Bansal V 2018 One-pot Synthesis of Maghemite Nanocrystals Across Aqueous and Organic Solvents for Magnetic Hyperthermia *Applied Materials Today* **12** 250–259
- [39] Tadic M, Panjan M, Tadic BV, Lazovic J, Damnjanovic V, Kopani M and Kopanja L 2019 Magnetic Properties of Hematite ( $\alpha$ -Fe<sub>2</sub>O<sub>3</sub>) Nanoparticles Synthesized by Sol-gel Synthesis Method: The Influence of Particle Size and Particle Size Distribution *Journal of Electrical Engineering* **70** 71–76
- [40] Morales-Morales JA 2017 Synthesis of Hematite  $\alpha$ -Fe<sub>2</sub>O<sub>3</sub> Nano Powders by the Controlled Precipitation Method *Ciencia en Desarrollo* **8** 99-107
- [41] Yufanyi DM, Ondoh AM, Foba-Tendo J and Ketcha Joseph Mbadcam 2015 Effect of Decomposition Temperature on the Crystallinity of  $\alpha$ -Fe<sub>2</sub>O<sub>3</sub> (Hematite) Obtained from an Iron(III)-Hexamethylenetetramine Precursor *American Journal of Chemistry* **5** 1-9
- [42] Esmael Darezereshki 2011 One-step Synthesis of Hematite ( $\alpha$ -Fe<sub>2</sub>O<sub>3</sub>) Nano-Particles by Direct Thermal-Decomposition of Maghemite *Materials Letters* **65** 642–645
- [43] Al-Gaashani R, Radiman S, Tabet N and Daud A R 2011 Rapid Synthesis and Optical Properties of Hematite ( $\alpha$ -Fe<sub>2</sub>O<sub>3</sub>) Nanostructures Using a Simple Thermal Decomposition Method *Journal of Alloys and Compounds* **550** 395–401
- [44] Djordje Trpkov, Matjaž Panjan, Lazar Kopanja and Marin Tadic 2018 Hydrothermal Synthesis, Morphology, Magnetic Properties and Self-Assembly of Hierarchical  $\alpha$ -Fe<sub>2</sub>O<sub>3</sub> (hematite) Mushroom-, Cube- and Sphere-like Superstructures *Applied Surface Science* **457** 427–438
- [45] Marin Tadic, Djordje Trpkov, Lazar Kopanja, Sandra Vojnovic and Matjaz Panjan 2019 Hydrothermal Synthesis of Hematite ( $\alpha$ -Fe<sub>2</sub>O<sub>3</sub>) Nanoparticle Forms: Synthesis Conditions, Structure, Particle Shape Analysis, Cytotoxicity and Magnetic Properties *Journal of Alloys and Compounds* **792** 599-609
- [46] Li-Hong Han, Hui Liu and Yu Wei 2011 In Situ Synthesis of Hematite Nanoparticles Using a Low-Temperature Microemulsion Method *Powder Technology* **207** 42–46
- [47] Mohammad Reza Housaindokht and Ali Nakhaei Pour 2012 Study the Effect of HLB of Surfactant on Particle Size Distribution of Hematite Nanoparticles Prepared Via the Reverse Microemulsion *Solid State Sciences* **14** 622-625
- [48] Amir Hassanjani-Roshan, Mohammad Reza Vaezi, Ali Shokuhfar and Zohreh Rajabali 2011 Synthesis of Iron Oxide Nanoparticles Via Sonochemical Method and Their Characterization *Particuology* **9** 95–99
- [49] Mihail Lacob 2015 Sonochemical Synthesis of Hematite Nanoparticles *Chemistry Journal of Moldova. General, Industrial and Ecological Chemistry* **10** 46-51
- [50] Hana Ovcaciková, Jozef Vlcek, Vlastimil Matejka, Jan Jurica, Petra Maierová and Petr Mlcoch 2020 The Effect of Temperature and Milling Process on Steel Scale Utilized as a Pigment for Ceramic Glaze *Materials* **13** 1814

- [51] Diah Eldin Fouad, Chunhong Zhang, Tadele Daniel Mekuria, Changlong Bi, Asad A. Zaidi and Ahmer Hussain Shah 2019 Effects of Sono-Assisted Modified Precipitation on the Crystallinity, Size, Morphology, and Catalytic Applications of Hematite ( $\alpha$ -Fe<sub>2</sub>O<sub>3</sub>) Nanoparticles: A Comparative Study *Ultrasonics - Sonochemistry* **59** 104713
- [52] Vinayak Anand Kamat, Swaroop K, Kiran K U, Benny George and Somashekarappa H M 2019 Effects of Hematite-Lead Oxide Combination in Ethylene-Propylene-Diene-Monomer on Shielding 59.54keV Gamma Rays *Radiation Physics and Chemistry*, **156** 50-57
- [53] Amirreza Khataee, João Azevedo, Paula Dias, Dzmitry Ivanou, Emil Dražević, Anders Bentien and Adélio Mendes 2019 Integrated Design of Hematite and Dye-sensitized Solar Cell for Unbiased Solar Charging of an Organic-inorganic Redox Flow Battery *Nano Energy* **62** 832–843
- [54] Abd El Aal S A., Abdelhady A M, Mansour N A, Nabil M H, Fekry Elbaz and Elsayed K E 2019 Physical and Chemical Characteristics of Hematite Nanoparticles Prepared Using Microwave-assisted Synthesis and Its Application as Adsorbent for Cu, Ni, Co, Cd and Pb From aqueous Solution *Materials Chemistry and Physics* **235** 121771
- [55] Verma K C, Navdeep Goyal, Manpreet Singh, Mukhwinder Singh and Kotnala R K 2019 Hematite  $\alpha$ -Fe<sub>2</sub>O<sub>3</sub> Induced Magnetic and Electrical Behavior of NiFe<sub>2</sub>O<sub>4</sub> and CoFe<sub>2</sub>O<sub>4</sub> Ferrite Nanoparticles *Results in Physics* **13** 102212
- [56] Ponomar V P 2018 Synthesis and Magnetic Properties of Magnetite Prepared by Chemical Reduction from Hematite of Various Particle Sizes *Journal of Alloys and Compounds* **741** 28-34
- [57] Funari V, Mantovani L, Vigliotti L, Tribaudino M, Dinelli E and Braga R 2018 Superparamagnetic Iron Oxides Nanoparticles from Municipal Solid Waste Incinerators *Science of the Total Environment* **621** 687–696
- [58] Rajesh Kumar R, Rishav Raj and Venimadhav A 2019 Weak Ferromagnetism in Band-gap Engineered  $\alpha$ -(Fe<sub>2</sub>O<sub>3</sub>)<sub>1-x</sub> (Cr<sub>2</sub>O<sub>3</sub>)<sub>x</sub> Nanoparticle *Journal of Magnetism and Magnetic Materials* **473** 119–124
- [59] Elvira Fantechi, Alessandro Ponti and Anna M F 2020 Chapter 12 - Synthesis and Design of Ferro- and Ferrimagnetic NPs: Size and Shape Control in Wet-chemistry Synthesis *Advances in Nanostructured Materials and Nanopatterning Technologies* p 333-379
- [60] Jussi Tikkanen and Petriina Paturi 2014 Iron Oxide Nanocomposite Magnets Produced by Partial Reduction of Strontium Hexaferrite *EPJ Web of Conferences* **74** 04007
- [61] Suprapedi, Priyo Sardjono, Muljadi and Kerista Sebayang 2018 Influence Composition Fe<sub>2</sub>O<sub>3</sub> of Isotropic Magnet BaFe<sub>12</sub>O<sub>19</sub> on Microstructure and Magnetic Properties *IOP Conf. Series: Journal of Physics: Conf. Series* **1091** 012025
- [62] Li J, Zhang H F, Shao G Q, Chen D, Zhao G G, Gao Z S, Liu J H, Lu J S and Li X B 2015 Synthesis and Properties of New Multifunctional Hexaferrite *Powders Procedia Engineering* **102** 1885 – 1889
- [63] Pullar R C 2012 Hexagonal Ferrite: a Review of The Synthesis, Properties and Application of Hexaferrite Ceramics *Progress in Materials Science* **57** 1191-1334
- [64] El-Eskandarany MS 2001 *Mechanical Alloying for The Fabrication of Advanced Engineering Materials* (New Jersey: Noyes Publications)
- [65] Suryanarayana C 2004 *The Mechanical Alloying and Milling* (New York, Marcel Dekker)
- [66] Peng Long, Li Lezhong, Wang Rui, Tu Xiaoqiang and Hu Yun 2017 Low Temperature Sintering Characteristics of Hot Press Sintered SrFe<sub>12</sub>O<sub>19</sub> Ferrites for Use in Microwave LTCC Circulators *Rare Metal Materials and Engineering* **46** 0951-0954
- [67] Sadullahoglu G, Ertug B, Gokce H, Altunccevahir B, Ozturk M, Topkaya R, Akdogan N, Ovecoglu M L and Addemir O 2015 The Effect of Milling Time and Sintering Temperature on Crystallization of BaFe<sub>12</sub>O<sub>19</sub> Phase and Magnetic Properties of Ba-Hexaferrite Magnet *ACTA PHYSICA POLONICA A* **128** 377-382
- [68] Burhan Shafiqat M, Omer Arif, Shahid Atiq, Murtaza Saleem, Shahid M R, Asif Mahmood and Shahzad Naseem 2016 Influence of Sintering Temperature on Structural, Morphological and Magnetic Properties of Barium Hexaferrite Nanoparticles *Modern Physics Letters B* **1650254** 1-9
- [69] Venkateswarlu Annpureddy, Joo-Hee Kang, Haribabu Palneedi, Jong-Woo Kim, Cheol-Woo Ahn, Si-Young Choi, Scooter David Johnson and Jungho Ryu 2017 Growth of Self-Textured Barium Hexaferrite Ceramics by Normal Sintering Process and Their Anisotropic Magnetic Properties *Journal of the European Ceramic Society* **37** 4701-4706
- [70] Darko Makovec, Sašo Gyergyek, Tanja Goršak, Blaž Belec and Darja Lisjak 2019 Evolution of The Microstructure during the Early Stages of Sintering Barium Hexaferrite Nanoplatelets *Journal of the European Ceramic Society* **39** 4831–4841
- [71] Kristiantoro, Idayanti, Dedi, Sudrajat, Mulyadi and Gustinova 2019 Influence of Compaction

Pressure on Magnetic Characteristics, Density, and Hardness of Barium Hexaferrite *IOP Conf. Series: Materials Science and Engineering* **620** 012106

- [72] Kools F 1992 *Hard Ferrites. Concise Encyclopedia of Magnetic & Superconducting Materials*. **126** p 129 (Oxford: Pergamon Press)
- [73] Zhuravlev V A, Nevmyvaka A A, Itin V I, Svetlichnyi V A, Lapin I N and Wagner D V 2019 Influence of The Reagent Types on The Characteristics of Barium Hexaferrites Prepared by Mechanochemical Method *Materials Today Communications* **21** 100614

## artikel 5

---

### ORIGINALITY REPORT

---

17%

SIMILARITY INDEX

12%

INTERNET SOURCES

15%

PUBLICATIONS

7%

STUDENT PAPERS

---

### PRIMARY SOURCES

---

1	Submitted to Canadian University of Dubai Student Paper	3%
2	R D Widodo, Priyono, Rusiyanto, S Anis, A A Ichwani, B Setiawan, D F Fitriyana, L Rochman. "Synthesis and characterization of iron (III) oxide from natural iron sand of the south coastal area, Purworejo Central Java", Journal of Physics: Conference Series, 2020 Publication	3%
3	repo.ur.krakow.pl Internet Source	2%
4	19avocats.be Internet Source	1%
5	pt.scribd.com Internet Source	1%
6	Repository.Unej.Ac.Id Internet Source	1%
7	Marin Tadic, Matjaz Panjan, Biljana Vucetic Tadic, Jelena Lazovic, Vesna Damnjanovic, Martin Kopani, Lazar Kopanja. " Magnetic	1%

properties of hematite ( – Fe O ) nanoparticles synthesized by sol-gel synthesis method: The influence of particle size and particle size distribution ", Journal of Electrical Engineering, 2019

Publication

8

I Safitri, Y G Wibowo, D Rosarina, Sudibyو. " Synthesis and characterization of magnetite (Fe O ) nanoparticles from iron sand in Batanghari Beach ", IOP Conference Series: Materials Science and Engineering, 2021

Publication

1 %

9

Plonczak, P.. "Fabrication of solid oxide fuel cell supported on specially performed ferrite-based perovskite cathode", Journal of Power Sources, 20080615

Publication

1 %

10

[dr.rgf.bg.ac.rs](http://dr.rgf.bg.ac.rs)

Internet Source

1 %

11

Submitted to National Institute of Technology, Rourkela

Student Paper

1 %

12

Marin Tadic, Djordje Trpkov, Lazar Kopanja, Sandra Vojnovic, Matjaz Panjan.

"Hydrothermal synthesis of hematite ( $\alpha$ -Fe<sub>2</sub>O<sub>3</sub>) nanoparticle forms: Synthesis conditions, structure, particle shape analysis,

< 1 %

cytotoxicity and magnetic properties", Journal of Alloys and Compounds, 2019

Publication

13

[ikee.lib.auth.gr](http://ikee.lib.auth.gr)

Internet Source

<1 %

14

Wirdati Mardhatillah, Erwin Amiruddin, Erman Taer. "Composition Modification of Iron Oxide Particles Using Activated Carbon for Adsorbtion of Cooper-Polluted Water From Siak River Water Pekanbaru, Riau", Journal of Physics: Conference Series, 2020

Publication

<1 %

15

[www.mdpi.com](http://www.mdpi.com)

Internet Source

<1 %

16

[www.researchgate.net](http://www.researchgate.net)

Internet Source

<1 %

17

[yoksis.bilkent.edu.tr](http://yoksis.bilkent.edu.tr)

Internet Source

<1 %

18

Alireza Nouri, Cuie Wen. "Surfactants in Mechanical Alloying/Milling: A Catch-22 Situation", Critical Reviews in Solid State and Materials Sciences, 2013

Publication

<1 %

19

C.N.C. Hitam, A.A. Jalil. "A review on exploration of Fe<sub>2</sub>O<sub>3</sub> photocatalyst towards degradation of dyes and organic

<1 %

# contaminants", Journal of Environmental Management, 2020

Publication

20

Widiyastuti, Heru Setyawan, Mahardika F. Rois, Hariyati Purwaningsih, Puspita Nurlilasari. " MnO Nanoparticles Prepared by Alternating Monopolar Arrangement Electrolysis and Their Electrochemical Performances ", IOP Conference Series: Materials Science and Engineering, 2020

Publication

<1 %

21

[atrium.lib.uoguelph.ca](http://atrium.lib.uoguelph.ca)

Internet Source

<1 %

22

[autodocbox.com](http://autodocbox.com)

Internet Source

<1 %

23

[onlinelibrary.wiley.com](http://onlinelibrary.wiley.com)

Internet Source

<1 %

Exclude quotes On

Exclude matches Off

Exclude bibliography On

# artikel 5

---

GRADEMARK REPORT

---

FINAL GRADE

**/0**

GENERAL COMMENTS

**Instructor**

---

PAGE 1

---

PAGE 2

---

PAGE 3

---

PAGE 4

---

PAGE 5

---

PAGE 6

---

PAGE 7

---

PAGE 8

---

PAGE 9

---

PAGE 10

---